

Supporting Information

Thermosensitive Nanoplatform for Photoacoustic Imaging and NIR Light

Triggered Chemo-photothermal Therapy

Zikang Chen,^{†,‡} Yinuo Tu,[§] Di Zhang,[†] Chuang Liu,[†] Yuping Zhou,^{†,‡} Xiang Li,[§] Xu Wu,[§]

Ruiyuan Liua,^{†,‡,}*

[†] School of Biomedical Engineering, Southern Medical University, Guangzhou, 510515, P.R.

China

[‡] School of Pharmaceutical Sciences, Southern Medical University, Guangzhou, 510515, P.R.

China

[§] Department of Thoracic Surgery, Huiqiao Medical Center, Nanfang Hospital, Southern

Medical University, Guangzhou, 510515, P.R. China

*Corresponding author:

Tel:+86-20-62747496

Fax: +86-20-62789343

E-mail: ruiyliu@smu.edu.cn

Contents

Scheme S1. Synthetic route of C720.

Figure S1. ^1H NMR(400 MHz, CDCl_3) of heptan-3-yl-2-cyano-2-(4-(4-nitrophenyl)thiazol-2-yl)acetate.

Figure S2. ^{13}C NMR(100 MHz, CDCl_3) of heptan-3-yl-2-cyano-2-(4-(4-nitrophenyl)thiazol-2-yl)acetate.

Figure S3. IR spectrum of heptan-3-yl-2-cyano-2-(4-(4-nitrophenyl)thiazol-2-yl)acetate.

Figure S4. ^1H NMR (400 MHz, $\text{DMSO}-d_6$) of C720.

Figure S5. ^{13}C NMR (100 MHz, $\text{DMSO}-d_6$) of C720.

Figure S6. IR spectrum of C720.

Figure S7. Photothermal heating curves of C720 (50, 100, 200, 400 μM) under 808 nm NIR laser irradiation (2 W/cm^2 , 10 min).

Figure S8. Laser-density-dependent temperature elevation of C720 (100 μM) under 808 nm NIR laser irradiation (1.5, 2, 2.5, 3 W/cm^2 , 10 min).

Figure S9. (A) Time constant for heat transfer of C720. (B) Time constant for heat transfer of water. (C) Photothermal on/off cycle curve corresponding to the time constant of C720 and (D) water.

Figure S10. Temperature profiles of C720 aqueous dispersion (100 μM) for five laser on/off cycles.

Figure S11. Absorption spectra of C720 dispersion before and after NIR irradiation.

Figure S12. (A) Optimized conformation of C720. (B) HOMO and LUMO molecular orbitals of C720.

Figure S13. Fluorescence spectra of free C720 and C720 encapsulated in CDSTL ($E_x = 685$ nm, $E_m = 700-900$ nm).

Figure S14. Photothermal heating curves of CDSTL (25, 50, 100, 200 μM) under 808 nm NIR laser irradiation (2 W/cm^2 , 10 min).

Figure S15. Laser-density-dependent temperature elevation of CDSTL (50 μM) under 808 nm NIR laser irradiation (1.5, 2, 2.5, 3 W/cm^2 , 10 min)

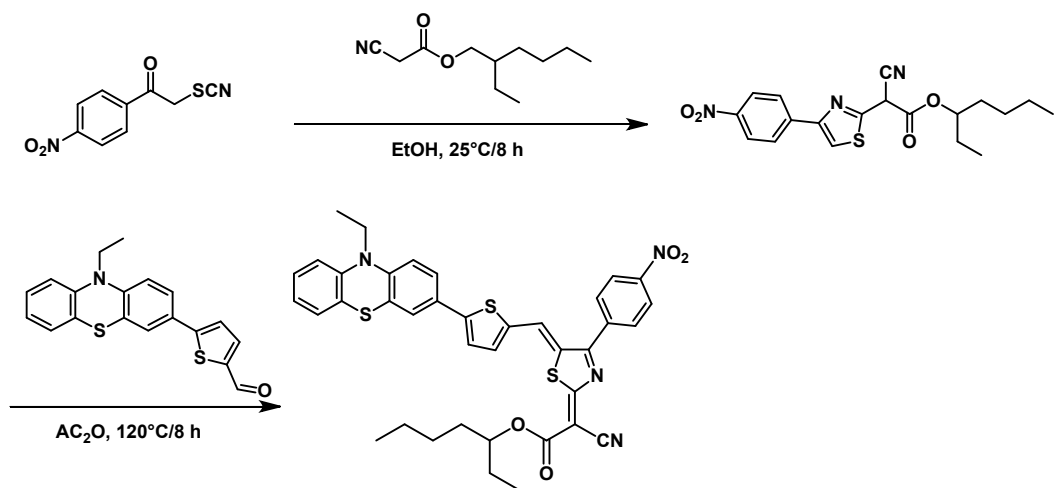
Figure S16. Temperature profiles of CDTSL (50 μ M) for four laser on/off cycles.

Figure S17. (A) Time constant for heat transfer of CDTSL. (B) Time constant for heat transfer of water. (C) Photothermal on/off cycle curve corresponding to the time constant of CDTSL and (D) water.

Figure S18. (A) PA images of SK-OV-3 tumor model after tail vein injection of CTSL or CDTSL. (B) PA signals of SK-OV-3 tumor model after tail vein injection of CTSL or CDTSL.

Figure S19. Histological analysis (Hematoxylin and Eosin staining) of organ slices treated mice after 14 days.

Calculation of photothermal conversion efficiency.



Scheme S1. Synthetic route of C720

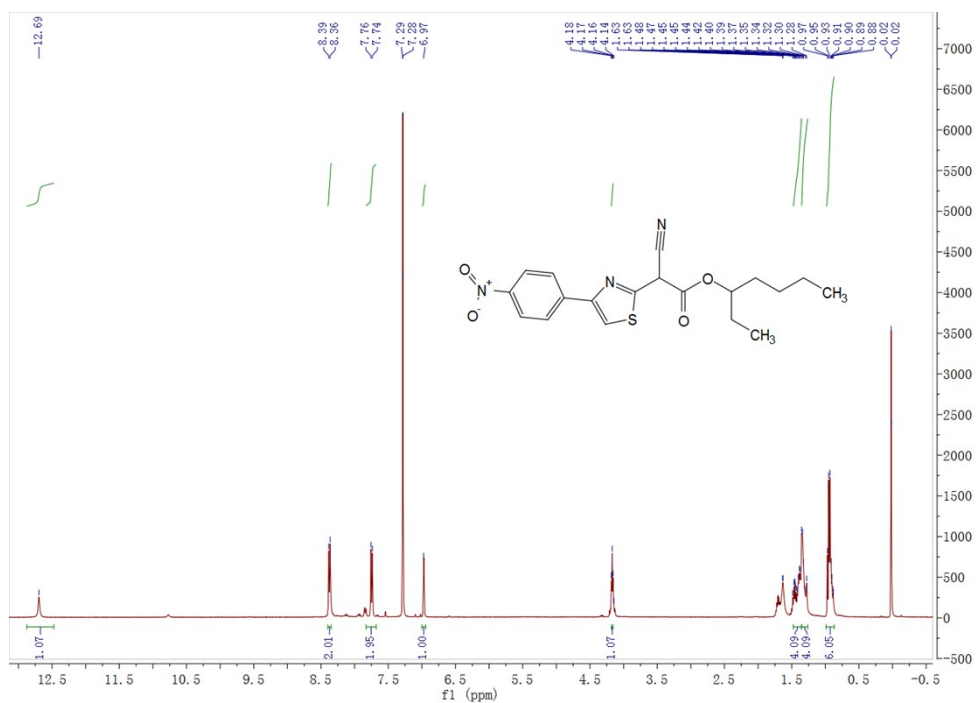


Figure S1. ¹H NMR (400 MHz, CDCl₃) of heptan-3-yl-2-cyano-2-(4-(4-nitrophenyl)thiazol-2-yl)acetate.

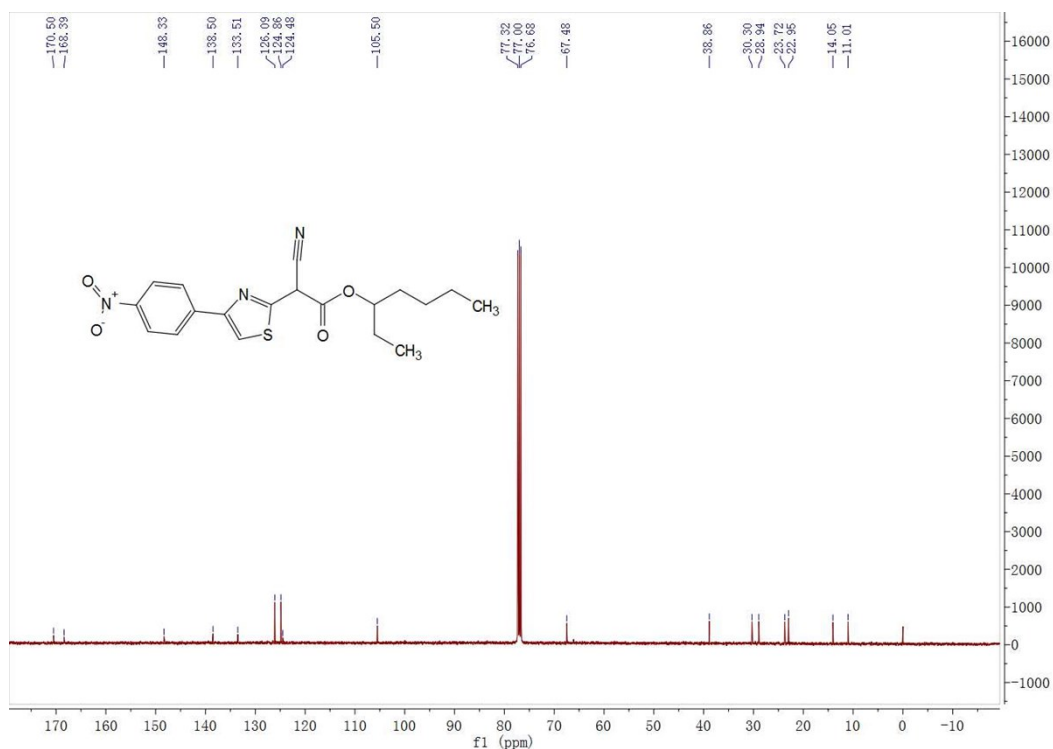


Figure S2. ^{13}C NMR (100 MHz, CDCl_3) of heptan-3-yl-2-cyano-2-(4-(4-nitrophenyl)thiazol-2-yl)acetate.

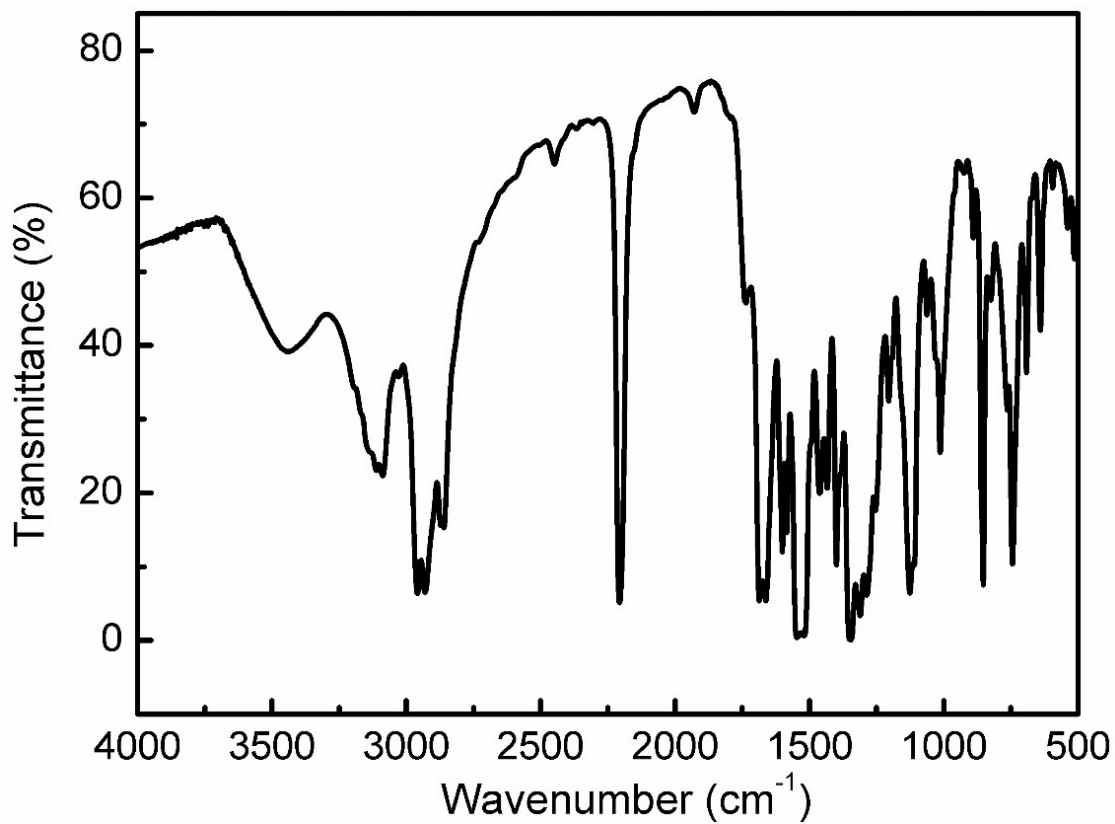


Figure S3. IR spectrum of heptan-3-yl-2-cyano-2-(4-(4-nitrophenyl)thiazol-2-yl)acetate.

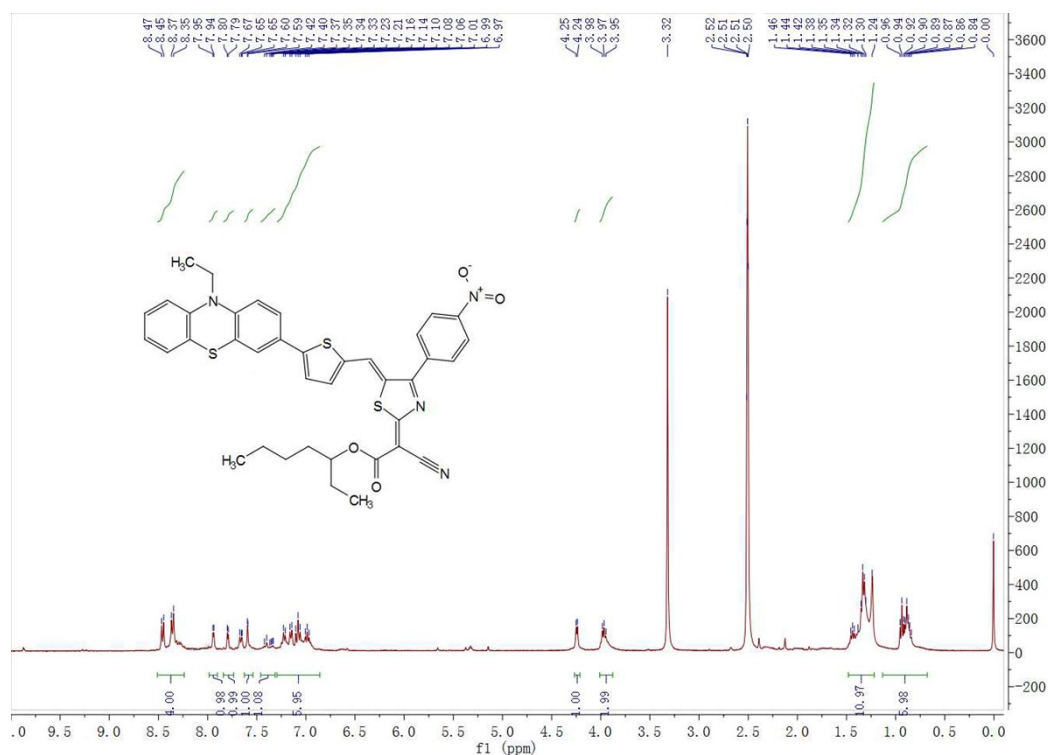


Figure S4. ^1H NMR (400 MHz, $\text{DMSO-}d_6$) of C720.

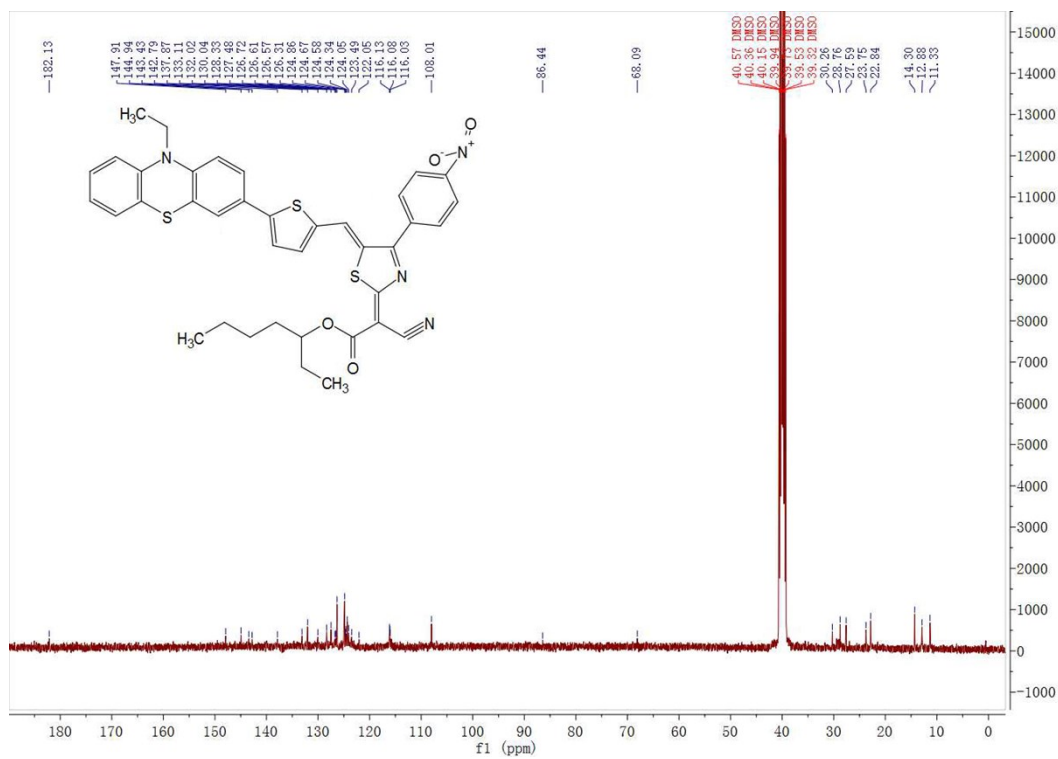


Figure S5. ^{13}C NMR (100 MHz, $\text{DMSO-}d_6$) of C720.

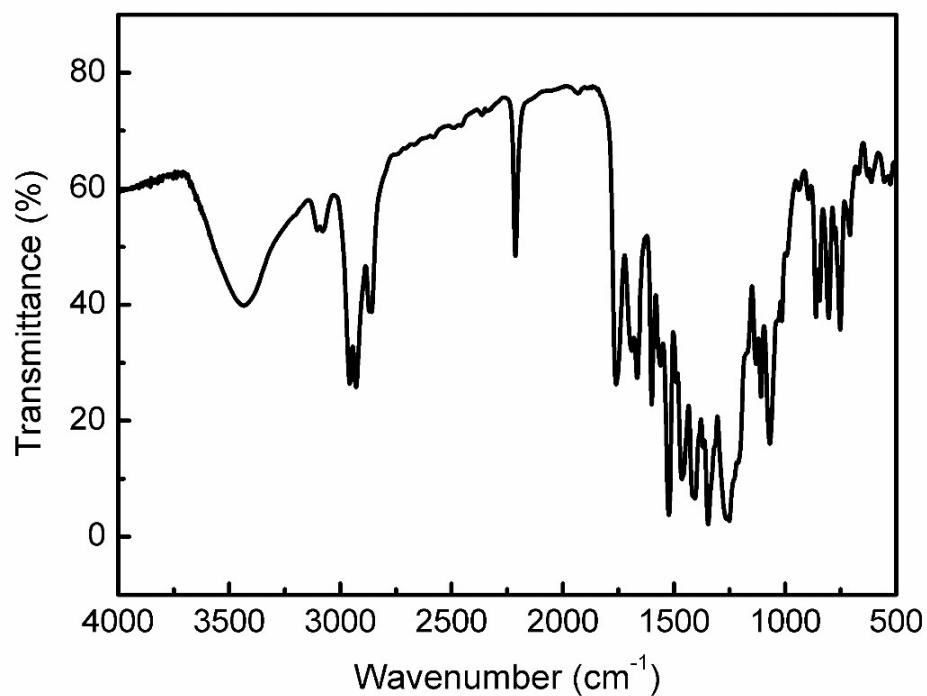


Figure S6. IR spectrum of C720

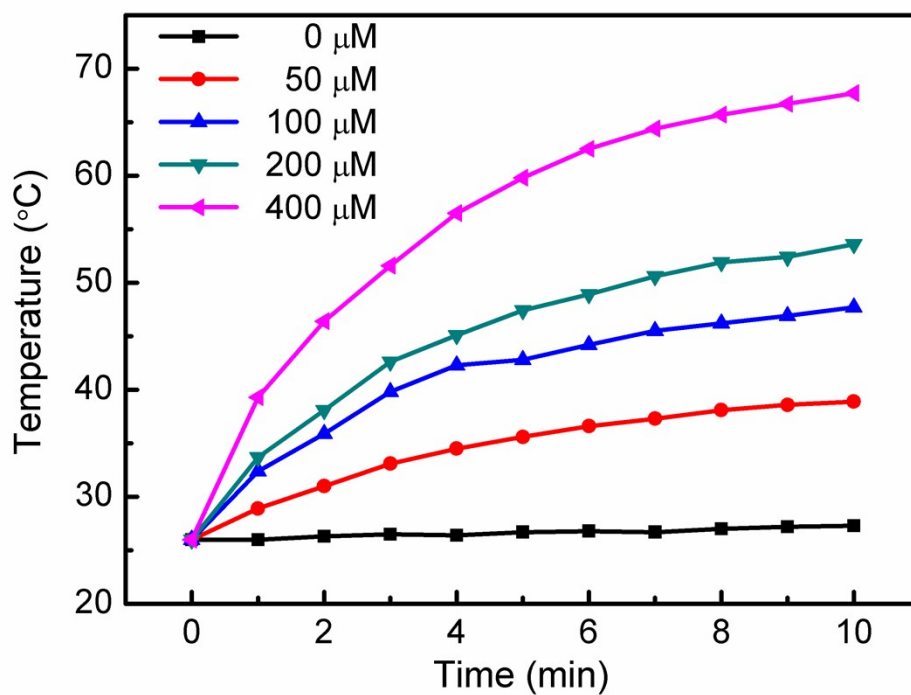


Figure S7. Photothermal heating curves of C720 (50, 100, 200, 400 μM) under 808 nm NIR laser irradiation (2 W/cm², 10 min).

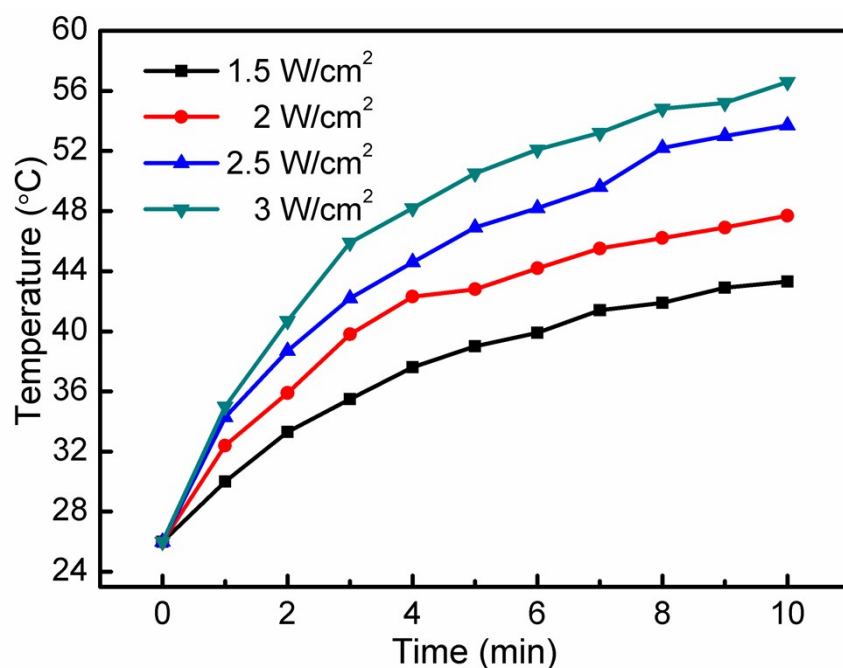


Figure S8. Laser-density-dependent temperature elevation of C720 (100 μM) under 808 nm NIR laser irradiation (1.5, 2, 2.5, 3 W/cm^2 , 10 min).

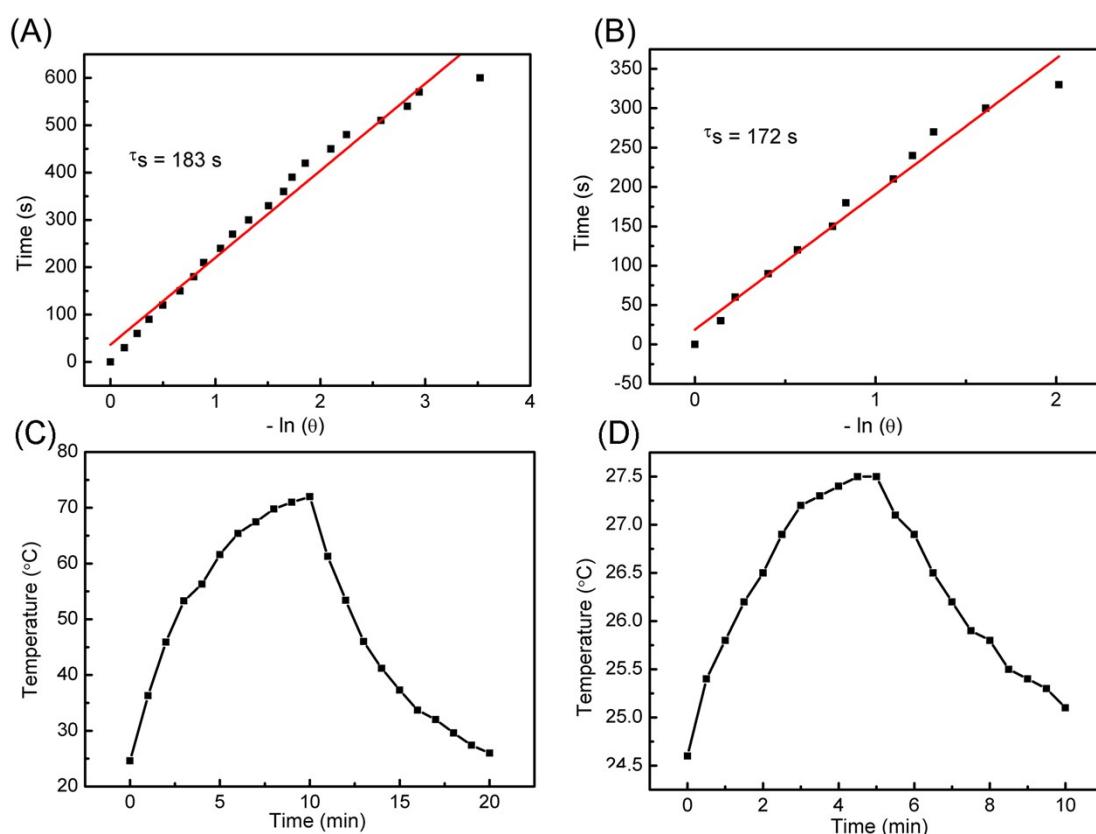


Figure S9. (A) Time constant for heat transfer of C720. (B) Time constant for heat transfer of water. (C) Photothermal on/off cycle curve corresponding to the time constant of C720 and (D) water.

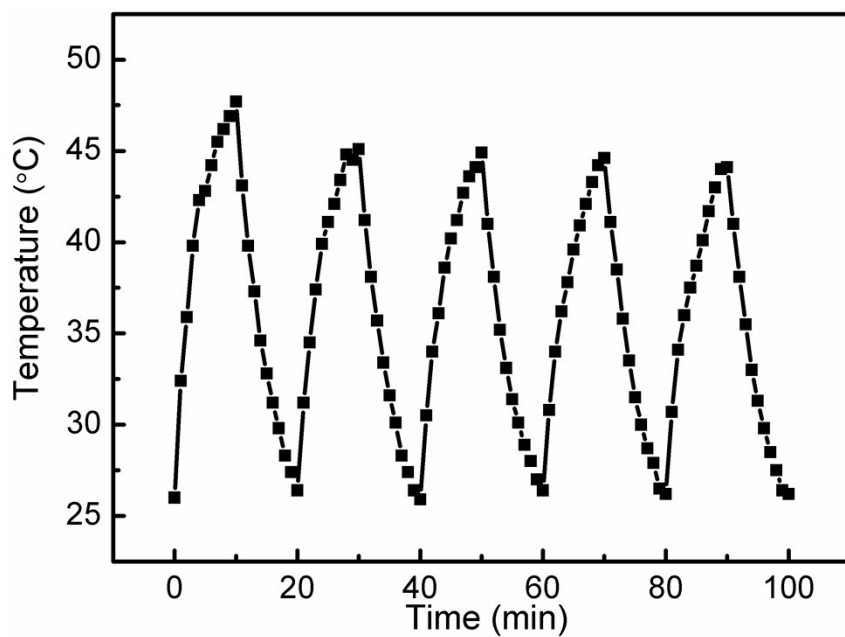


Figure S10. Temperature profiles of C720 aqueous dispersion (100 μM) for five laser on/off cycles.

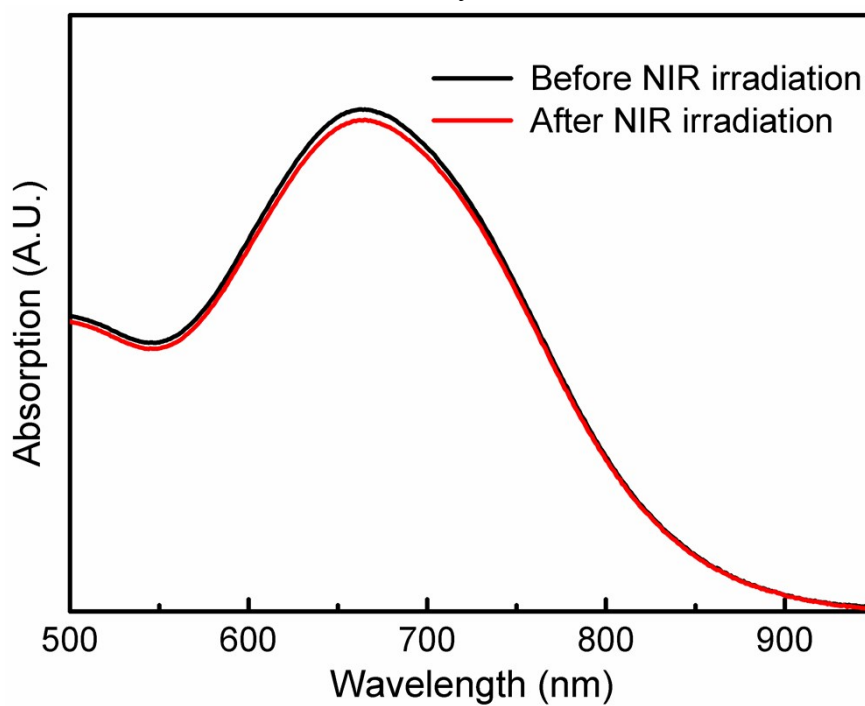


Figure S11. Absorption spectra of C720 dispersion before and after NIR irradiation.

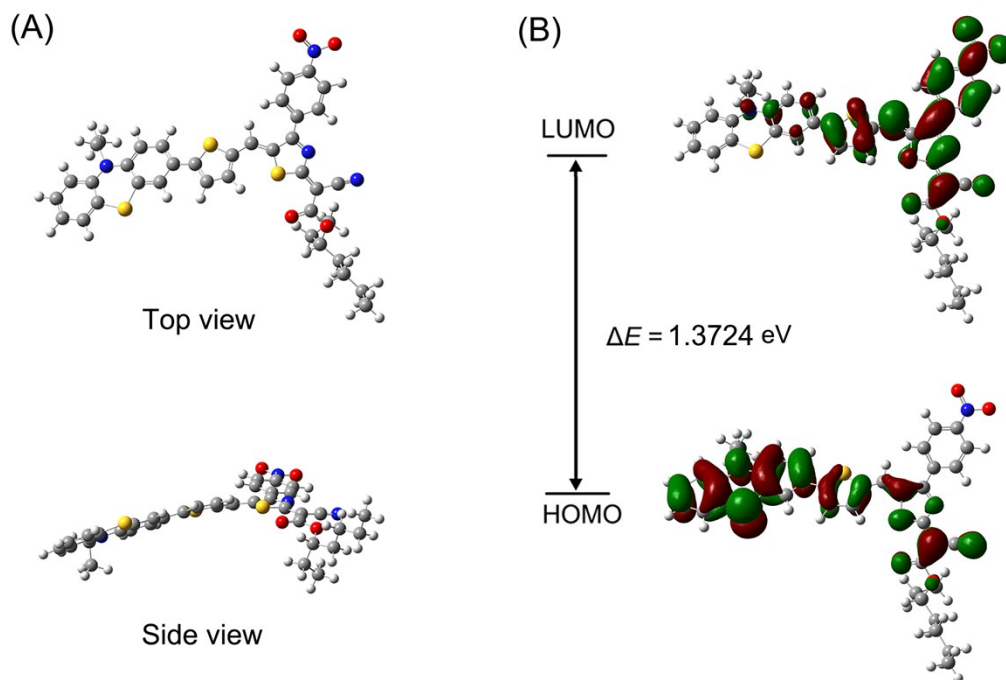


Figure S12. (A) Optimized conformation of C720. (B) HOMO and LUMO molecular orbitals of C720.

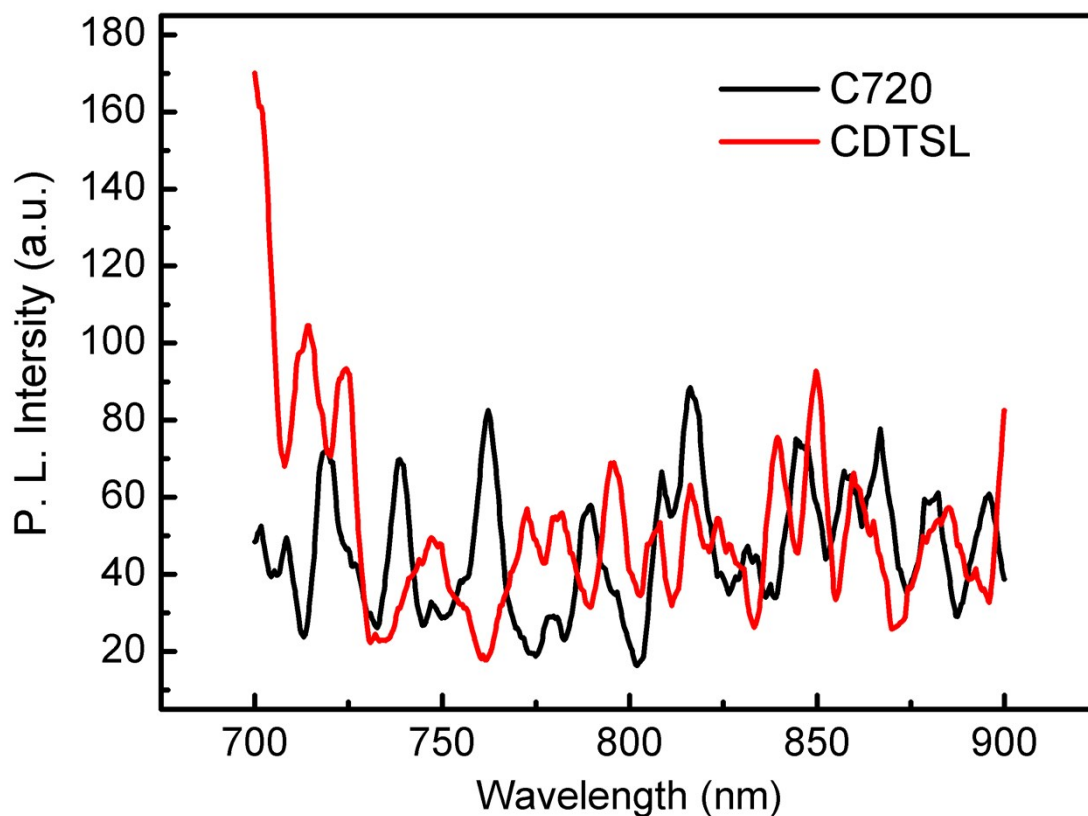


Figure S13. Fluorescence spectra of free C720 and C720 encapsulated in CDSTL ($E_x = 685 \text{ nm}$, $E_m = 700\text{-}900 \text{ nm}$).

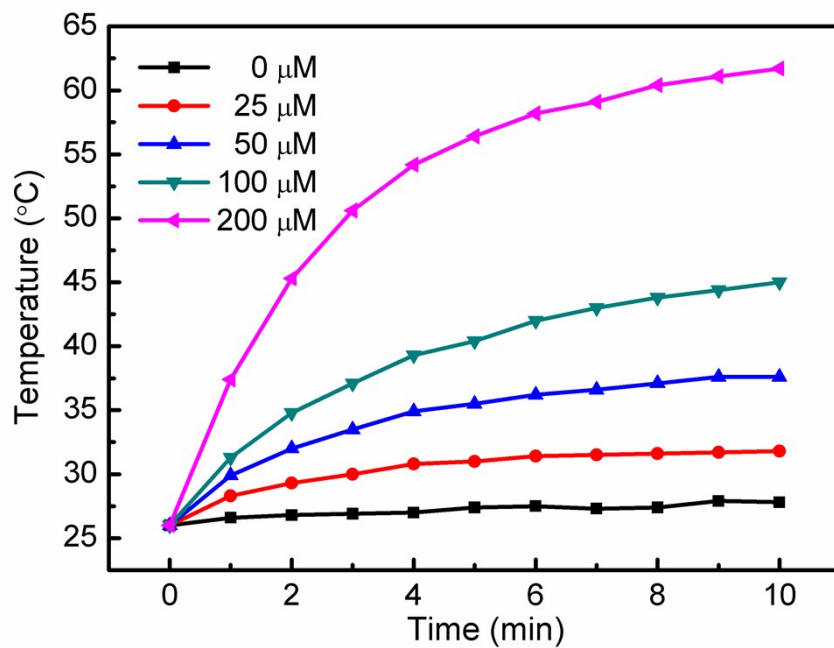


Figure S14. Photothermal heating curves of CDTSL (25, 50, 100, 200 μM) under 808 nm NIR laser irradiation (2 W/cm^2 , 10 min).

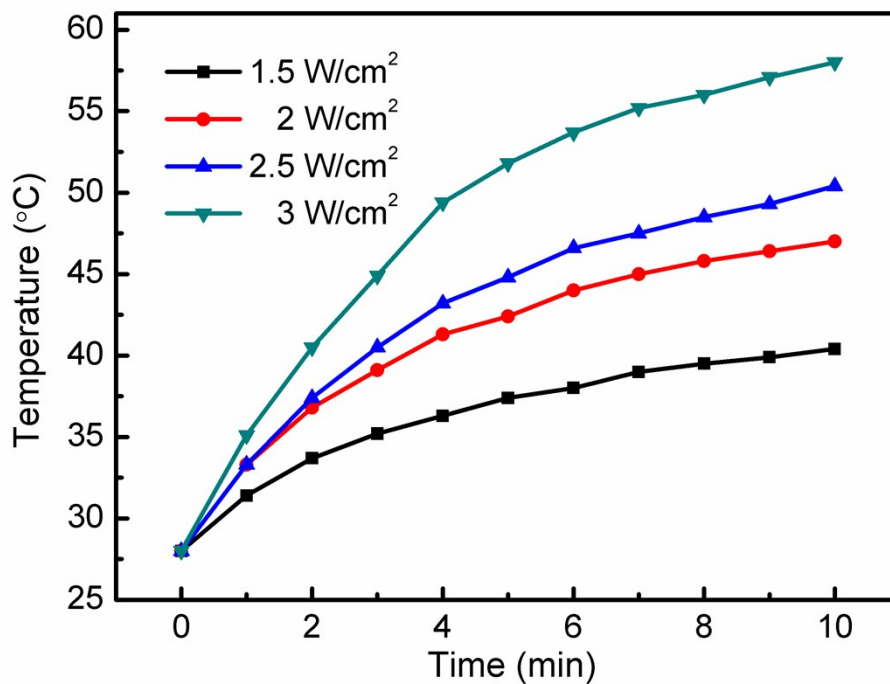


Figure S15. Laser-density-dependent temperature elevation of CDTSL (50 μM) under 808 nm NIR laser irradiation (1.5, 2, 2.5, 3 W/cm^2 , 10 min)

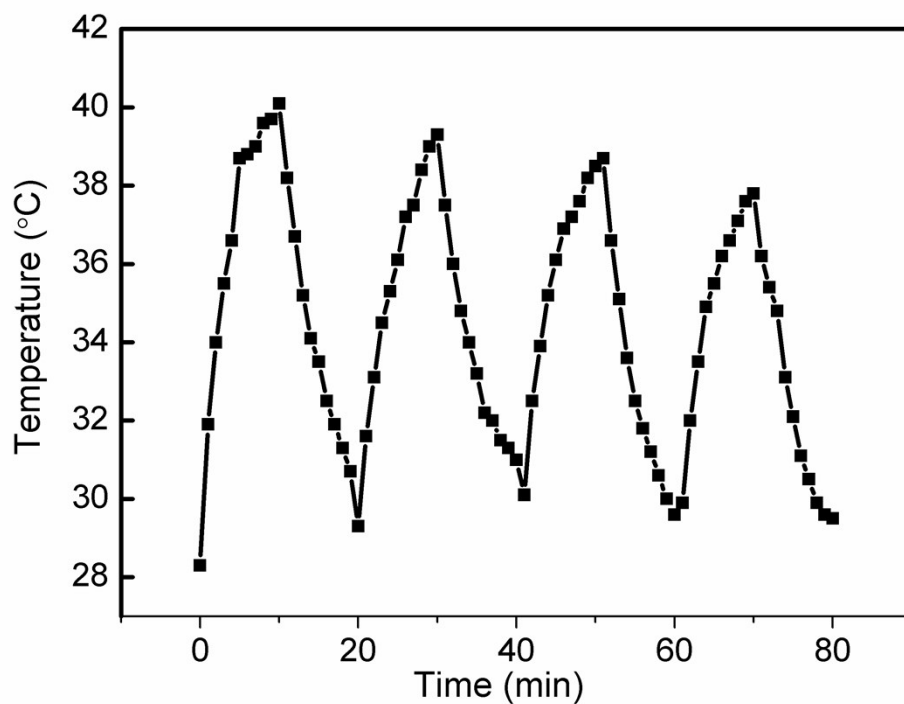


Figure S16. Temperature profiles of CDTSL (50 μ M) for four laser on/off cycles.

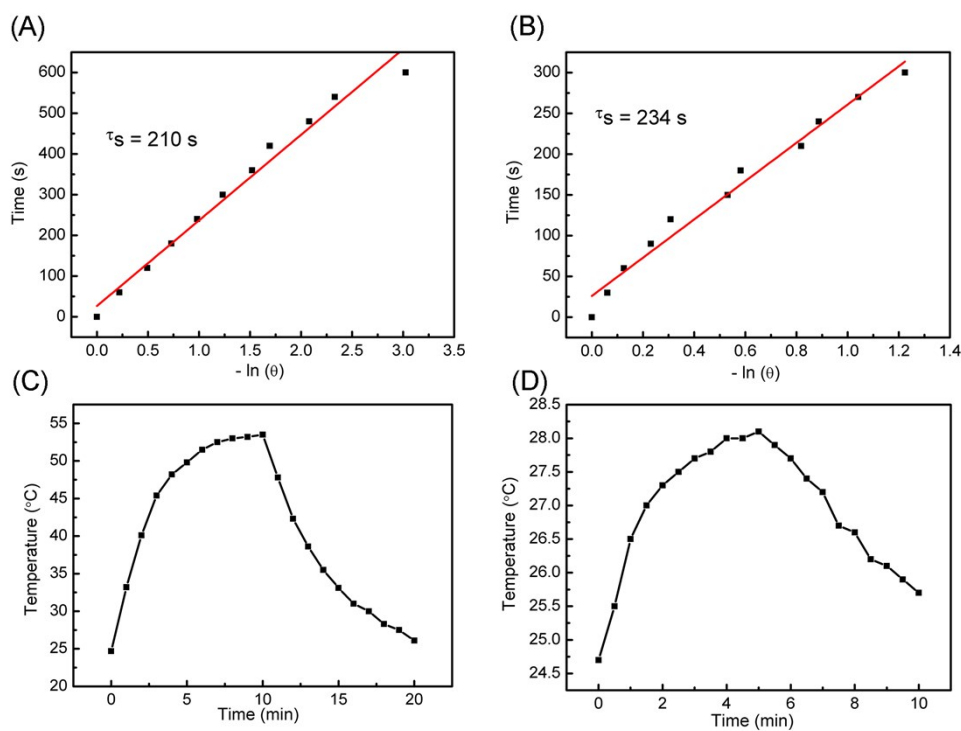


Figure S17. (A) Time constant for heat transfer of CDTSL. (B) Time constant for heat transfer of water. (C) Photothermal on/off cycle curve corresponding to the time constant of CDTSL and (D) water.

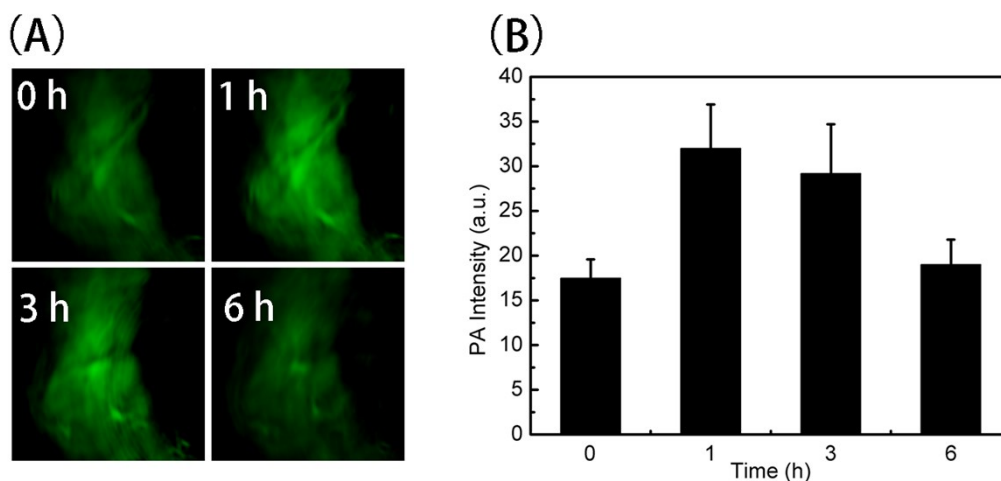


Figure S18. (A) PA images of SK-OV-3 tumor model after tail vein injection of CTSL or CDTSL. (B) PA signals of SK-OV-3 tumor model after tail vein injection of CTSL or CDTSL.

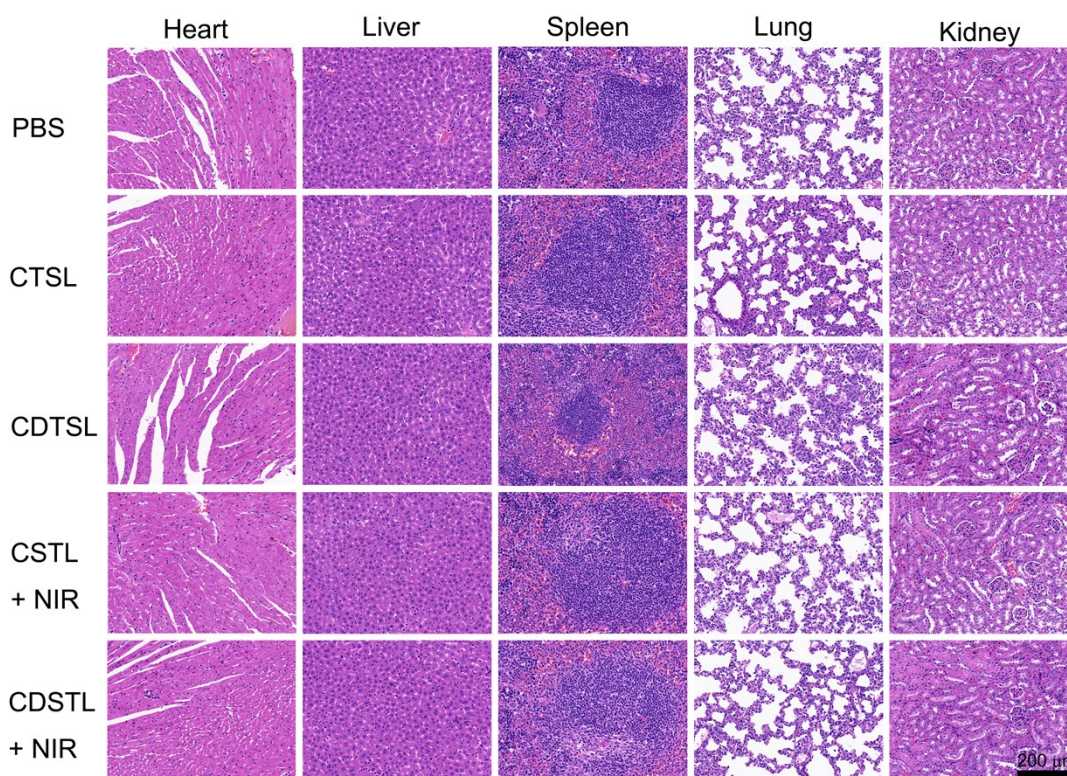


Figure S19. Histological analysis (Hematoxylin and Eosin staining) of organ slices treated mice after 14 days.

Calculation of photothermal conversion efficiency

The photothermal conversion efficiency of C720 was calculated by measuring the temperature change of the C720 aqueous as a function of time under continuous

irradiation with an 808 nm laser (3 W cm^{-2}) for 600 s (t) until the temperature of the solution reached a steady-state. The photothermal conversion efficiency (η) was calculated by eqn (1),

$$\eta = [hA(T_{\max} - T_{\text{surr}}) - Q_{\text{Dis}}] / [I(1 - 10^{-A\lambda})] \quad (1)$$

where h is the heat transfer coefficient, A is the area of the container, T_{\max} is the maximum steady-state temperature (72°C), T_{surr} is the ambient temperature of the environment (24.6°C), Q_{Dis} represents the heat dissipation from the light absorbed by the solvent and the sample cell, I is the incident laser power (3 W cm^{-2}), and $A\lambda$ is the absorbance of the sample at 808 nm (0.342). The value of hA was calculated by eqn (2),

$$hA = m_{\text{D}}c_{\text{D}}/\tau_{\text{s}} \quad (2)$$

where τ_{s} is the time constant for the heat transfer in the system, which was accessed based on the measurements in Figure S9 ($\tau_{\text{s}} = 183 \text{ s}$); and m_{D} and c_{D} are the mass (1 g) and heat capacity (4.2 J g^{-1}) of DI water used to disperse the C720, respectively. The photothermal conversion efficiency of C720 was calculated to be 62%.

For calculation of photothermal conversion efficiency of CDTSL, $T_{\max} = 53.5^\circ\text{C}$, $T_{\text{surr}} = 24.7^\circ\text{C}$, $I = 3 \text{ W cm}^{-2}$, $A\lambda = 0.1486$, $\tau_{\text{s}} = 210 \text{ s}$ (Figure S13), $\eta = 59\%$.